Table of contents

Identifying the Pollution Characteristics of Atmospheric Polycyclic Aromatic Hydrocarbons Associated with Functional districts in Ningbo, China

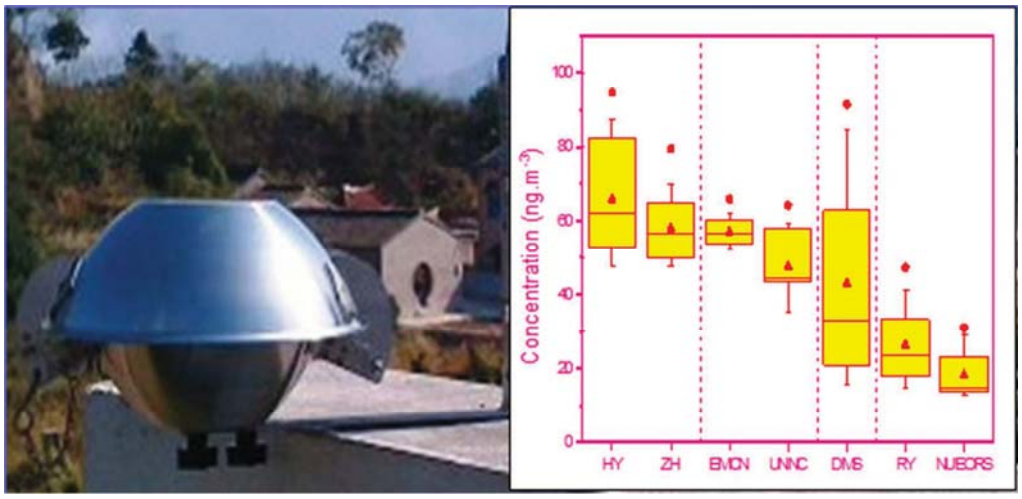

Hydrocarbons Associated with Functional districts in Ningbo, China

Cheng-Hui Peng[1,2,3,a], Lei Tong[1,3,a], Zhong-Wen Huang[1,2,3], Jing-jing Zhang[1,2,3], Hang Xiao[1,3*], Neng-Bin Xu[4], Jun He[5]

[1] Center for Excellence in Regional Atmospheric Environment, Institute of Urban Environment, Chinese Academy of Sciences, Xiamen 361021, China

[2] University of Chinese Academy of Sciences, Beijing 100049, China

[3] Ningbo Urban Environment Observation and Research Station-NUEORS, Chinese Academy of Sciences, Ningbo 315830, China

[4] Environment monitoring Center of Ningbo, Ningbo 315012, China

[5] University of Nottingham Ningbo China, Ningbo 315100, China

[*]Correspondence author: Hang Xiao

Institutes of Urban Environment, Chinese Academy of Sciences

1799 Jimei Avenue, Xiamen, China, 361021

E-mail address: hxiao@iue.ac.cn

Tel: + 86 574 8678 4813

a, The two authors contributed equally to this paper.

Duplicate polyurethane foam based passive air sampler (PUF-PAS) were deployed in Ningbo at seven sites from November 2014 to October 2015 and analyzed for 16 priority polycyclic aromatic hydrocarbons (PAHs). The mean concentrations of Σ_{15}PAHs (except for naphthalene) were 45.3 ng/m^3 during the sampling period. The B[a]Peq concentration shows a slight seasonal variation with higher value observed in winter. Significant seasonal difference was observed among the sampling sites, which may be due to the emission characteristics of different functional areas. The highest annual mean concentration was found in industrial area (66 ± 18 ng/m^3). Correspondence analysis (CA) was used to characterize the PAH congener profiles associated with each functional district and their temporal variations. It shows that difference PAH composition profiles and seasonal variations were observed in mountain, rural area and residential areas; and different industrial layout also led to different property of PAH congener emission. Higher levels of PAHs were observed around oil refinery in summer and at mountainous areas in winter, which might attribute to the evaporation of petroleum and the impacts of local coal/biomass burning. Both CA and diagnostic ratio analysis indicates that Ningbo is likely influenced by both gasoline/diesel combustion and coal/biomass burning.

Keywords: Polycyclic aromatic hydrocarbons (PAHs); Passive air sampling; Seasonal variations; Ningbo.

1. Introduction

Polycyclic aromatic hydrocarbons (PAHs), which belong to the group of semi-volatile organic compounds (SVOCs), are ubiquitously observed in ambient air. They have been received much attention due to their carcinogenic, mutagenic properties, which could cause negative health effects if they were inhaled by people [1]. PAHs can be emitted from both the natural and anthropogenic sources through incomplete combustion. Anthropogenic source includes biomass and coal combustion for heating and industry activities[2]. Some natural activities could also release a considerable amount of PAHs, such as volcanic eruptions and forest fires[3]. Therefore, United States Environmental Protection Agency (USEPA) has listed 16 PAHs as priority

and this value entered in to force in 2012[4] .

In previous studies, SVOCs were usually collected with active air samplers (AAS) techniques, which were considered to be one of the most accurate methods [5]. However, AAS needs power supply and therefore are limited in their application. Compared to AAS, passive air samplers (PAS) has the advantage of easy handling, cost effective and no power supply requirement. Over the past decades, polyurethane foam (PUF) disk [6], XAD-resin [7], sorbent-impregnated polyurethane foam (SIP)[8] and semi-permeable membrane devices (SPMD) [9, 10] based PAS have been widely deployed in different areas to study the spatial distribution and transportation of SVOCs. In the past decades, the PUF passive air sampler (PUF-PAS) are frequently used to monitor SVOCs and have been applied to study the ambient air concentration and long range atmospheric transport (LRAT) of SVOCs all over the world. Previous studies have already demonstrated that PAS was a reliable tool to study the urban-rural trends of POPs [11]. For example, PUF-PAS has been used to monitor SVOCs in the Global Atmospheric Passive Sampling (GAPS) project [12] and the Asian Soil and Air Monitoring Program [13].

China is the largest emitter of PAHs in the world. With the development of economy, a large amount of PAHs were emitted from all over the world, especially in China. Shen et al. estimated that the global total atmospheric emission of 16 PAHs was 504 Gg in 2007 [14]. In 2007, the annual emission of PAHs in China was about 106 Gg, accounting for 21% of the global total emission. The Yangtze River Delta (YRD), one of the most developed areas in East China, has large quantities of PAH emission [15]. Ningbo is situated at the south of YRD area. However, only a few studies have been conducted in Ningbo. For instance, Liu et al. [16] have studied the temporal variation of PAHs in the Ningbo Atmosphere Environment Observatory (NAEO) from July 2009 to March 2010 and Xu et al. [17] have studied the PAHs during heavy aerosol pollution period and low pollution period in the University of Nottingham Ningbo China (UNNC) from December 2012 to June 2013.

In this study, we intended to provide the detailed information of PAHs at different function districts in Ningbo using PUF-PAS techniques. The objectives of this study are: 1) to quantify the concentrations of PAHs in Ningbo from November 2014 to October 2015; 2) to study the spatial and temporal variation of PAHs in

assess human health risk to in Ningbo.

2. Materials and methods

2.1 Study area

As a famous port city, Ningbo is strongly influenced by the Siberia-Pacific monsoon with a hot and humid summer under the influence of Pacific monsoon and a cold and dry winter under the influence of Siberia monsoon. Fig. 1 shows the specific location of the sampling sites. The sampling campaign started from October 31, 2014 and ended in October 30, 2015. Efforts were made on choosing the sampling sites to cover all sorts of the land-use areas. Based on the specific locations, the sampling sites are classified into four categories: residential site, industrial site, mountain site and rural site.

(1) Residential site includes the Environment Monitoring Center of Ningbo (EMCN) and the University of Nottingham Ningbo China (UNNC). The EMCN site is situated in the city center and surrounded by a lot of residential buildings. Domestic coal burning as well as traffic emission contributes to the sampling sites. The UNNC site is located at the south of the city, at least several miles away from the city center.

(2) Industrial site includes Zhen-Hai (ZH) and Heng-Yang (HY) site. ZH site is located at the dormitory of Zhen-Hai Oil Refining. HY sites is located at industrial district where thermal power plant. Both sampling sites are closed to the highway road.

(3) The rural site includes Rui-Yan (RY) site and the Ningbo Urban Environment Observation and Research Station (NUEORS) site. RY site is located at the Center of Rui-Yan Country. The NUEORS site is situated at a coastal area.

(4) The Da-Mei-Shan (DMS) site is located at the summit of Da Mei Mountain in a remote area, at least 10 miles far away from the populated area and 20 miles away from the city areas, and is surrounded by forests. Some factories are distributed at the foot of the mountain.

2.2 PUF disk Preparation and Extraction

Prior to deployment, PUF disks were cleaned progressively by acetone, petroleum ether/ acetone (75:25), petroleum ether and acetone using an Accelerated Solvent

transferred to glass jars with Teflon lids until sampling. PUF disks were kept at 4 □ before transporting to the sampling sites. Duplicated PUF disk were deployed at seven sites in Ningbo for a month and 180 samples were collected in total. Once harvested, the PUF disks were stored under -20 □ until extraction. The PUF extraction process was as follows: PUF disks were extracted individually by hexane/acetone (3:1) using an ASE instrument. The extracts were then rotary evaporated, dehydrated and solvent exchanged to isooctane. All extracts were rotary evaporated under vacuum and then transferred to a vial, reduced under gentle nitrogen flow to 1 ml. The extracts were spiked with 20 ng of three internal standards (acenaphthene-d_{10}, pyrene-d_{10}, benzo[e]pyrene-d_{10}) and were stored at -20 □ until analysis.

2.3 Sample analysis

16 US-EPA-listed priority PAHs congeners are analyzed. They are: naphthalene (NAP), acenaphthylene (ACY), acenaphthene (ACE), fluorene (FLU), phenanthrene (PHE), anthracene (ANT), fluoranthene (FLT), pyrene (PYR), benzo[a]anthracene (BaA), chrysene (CHR), benzo[b]fluoranthene (BbF), benzo[k]fluoranthene (BkF), benzo[a]pyrene (BaP), dibenz[a,h]anthracene (DBA), indeno[1,2,3-cd]pyrene (IcdP), benzo[ghi]perylene (BghiP). PAHs standards were purchased from AccuStandard (New Haven, CT, USA) and three internal standards (acenaphthene-d_{10}, pyrene-d_{10}, benzo[e]pyrene-d_{10}) were acquired from Cambridge Isotope Laboratories (Andover, MA, USA).

The PAHs analysis was performed using a gas chromatograph – mass spectrometry (GC-MS, Agilent 7890B-5977A, USA) equipped with an electron ionization (EI) ion source. Selective ion mode (SIM) was applied to the PAHs detection. Target compounds were separated with an HP-5MS (30 m × 0.25 mm × 0.25 μm) column. The GC temperature was programmed as follows: held at 80 ℃ for 2 min; 10 ℃ min^{-1} to 280 ℃; and held for 10 min. The GC injection port was held at 250 ℃ and operated at splitless mode at a flow rate of 1.0 ml/minute.

2.4 Quality Assurance/Quality Control (QA/QC)

All analytical procedures were monitored using strict quality assurance (QA) and quality control (QC). Solvents used here were chromatograph grade or higher. The

remove any absorbed carbonaceous compounds.

During the extraction, two clean PUF disks were spiked with 20 ng of 16 PAHs standards in order to access recoveries and were treated as real samples. In this study, the recoveries ranged from 70% to 110%. One experimental blank PUF disk was prepared for each batch of 10 samples. A field blank PUF sample was prepared for each month. Method detection limits (MDLs) were defined as mean value of experimental blanks samples plus 3 times standard deviation. MDLs were ranged from 1 pg/m^3 to 2 pg/m^3. The instrumental detection limits (IDLs) were determined as injection amount that corresponds to signal-to-noise value of 3:1. As naphthalene have a higher concentration in blank samples, it was not discussed in this study. The reported air concentrations of 15 PAHs were corrected by the field blank in this study.

2.5 Deriving air concentration

Automatic meteorological stations near the sampling sites were selected to get the temperature data. However, the temperature difference was fairly small for the seven sites as shown in Table S1. Therefore, a common temperature for each month is selected to calculate the effective air volume. The detail information for the sampling sites was listed in Table 1.

The air concentration of PAHs (C_{AIR}, ng/m^3) is derived from the air mass (M, ng/sample) on the PUF disk divided by the effective air volume (V_{AIR}, m^3) of each specific analyst. The effective air volume was calculated using the following equation which was given by Harner et al. [11]and Harner et al.[18]:

$$V_{AIR} = K'_{PUF-A} V_{PUF} \left(1 - \exp\left[\left(\frac{k_A}{K'_{PUF-A}}\right)\left(\frac{A_{PUF}}{V_{PUF}}\right)\right] t\right) \quad (1)$$

where V_{PUF} is the volume of PUF disks, k_A is the air-side mass transfer coefficient (m/d); t is the exposure time in days; A_{PUF} is the effective film thickness (m). The k_A value is the sampling rate (R, m^3/d) divided by the surface area of the PUF disk samples (365 cm^2). The K'_{PUF-A} is related to PUF-air coefficient partition. Deriving K'_{PUF-A} was calculated using an equation which was given by Shoeib et al.[19]:

$$\log K'_{PUF-A} = \rho(0.6366 \log K_{OA} - 3.1774) \quad (2)$$

where ρ is the density of PUF plug. K_{OA} is the value of octanol-air partition coefficient. K_{OA} value was calculated using an empirical equation which was given by Odabasi et al.[20]:

where T (K) is the average air temperature for the sampling period.

According to previous study, PUF may be used to collect both gas and particle phase PAHs[21]. Klanova et al. [22]found that PUF only collected 10% of particle PAHs in a background site. However, other study reported that there are no difference in the particle PAHs R-value, such as in tropical[23] or in industrial / urban sites[18]. In this study, we calculate effective air volumes using the sampling rate R-value of 3.5 m^3/d according to previous studies[13, 24].

2.6 Statistic analysis

All data analyses were done with Microsoft Excel and software SPSS 24.0 (SPSS Inc., USA) with Correspondence analysis (CA) and Mann-Whitney test. Mann – Whitney test was used to investigate statistic difference[25]. CA was performed to reduce variable and maintaining the original information. CA is similar to principal component analysis, but applies to categorical data. CA is a descriptive and exploratory methods designed to discover the cross-classified data containing some measure of correspondence [26].

2.7 Health risk assessment

The B[a]P equivalent (B[a]Peq) was used to estimate the health risk of PAHs mixture. It is calculated by multiplying the mass concentration of specific PAHs species with their corresponding toxic equivalent factor (TEF). TEF for each species were given by Nisbet[27]. The B[a]Peq of PAHs was calculated by the equation:

$$\mathrm{B[a]Peq} = 0.001(\mathrm{ACE} + \mathrm{ACY} + \mathrm{PHE} + \mathrm{FLU} + \mathrm{FLT}) + 0.01(\mathrm{ANT} + \mathrm{CHR} + \mathrm{BghiP}) + 0.1(\mathrm{BaA} + \mathrm{BbF} + \mathrm{BkF} + \mathrm{IcdP}) + \mathrm{BaP} + \mathrm{DBA}$$

If the individual PAH concentration was below the limit of detection (LOD), the value of B[a]Peq was considered to be zero. The carcinogenic potencies of 15 PAHs were estimated as the sum B[a]Peq of each PAHs.

3. Results and Discussion

3.1 Levels of PAH and profile of composition

In this study, the annual mean Σ_{15}PAHs concentration was 45.3 ng/m^3 (range from 11.6 ng/m^3 to 94.8 ng/m^3), which was lower than the value observed in Beijing-Tianjin (Σ_{25}PAHs, 202 ng/m^3 in summer) [28], North China Plain (Σ_{15}PAHs,

When comparing with foreign nations, it is slightly higher than the value observed in Toronto, Canada (Σ_{17}PAHs, range = 3.3 - 61.5 ng/m^3 in four seasons) [24] and Temuco, Chile (Σ_{15}PAHs, range = ND - 70 ng/m^3 in four seasons) [31].

Based on the vapor pressure of 15 PAH species, they were classified into three classes[32]. The three groups are: (1) light PAHs (lPAH) (ACY, ACE, FLU, PHE, ANT); (2) middle PAHs (mPAH) (FLT, PYR, BaA, CHR); (3) particulate PAHs (pPAH) (DBA, BkF, BbF, BaP, BghiP, IcdP). In this study, the most abundant congeners are PHE (20 ± 8.9 ng/m^3), FLT (8.8 ± 5.1 ng/m^3), FLU (6.1 ± 2.9 ng/m^3) and PYR (5.5 ± 3.5 ng/m^3), which accounted 45%, 18%, 14% and 11% for the average concentration of total PAH, respectively. Weather condition may influence the process of PUF captured PAHs, especially for particular-phase PAHs [33, 34].

3.2 Spatial distribution

Based on different category function districts, the box plot of total 15 PAHs concentration for the seven sites are displayed in Fig. 2. The mean concentrations of total PAHs were in the order of industrial (HY: 66 ± 18; ZH: 60 ± 17) > residential (UNNC: 48 ± 9.8; EMCN: 57 ± 4.5) > mountain (DMS: 43 ± 27) > rural (NUEORS: 18 ± 6.7; RY: 26 ± 11), respectively. Statistic difference (Mann-Whitney, $p < 0.05$) was found between the rural site (NUEORS and RY) and other sites. Higher concentration were generally observed in urban area (HY, ZH, UNNC and EMCN sites) while lower concentration observed in rural or remote area (DMS, NUEORS and RY sites). Similar results could also found in previous studies. For example, Motelay-Massei et al. [24] attribute higher PAHs concentration in urban areas to the cause of population densities. In residential areas, domestic combustion for heating and cooking are important PAHs source. Increasing wood burning during the heavy pollution periods was found In Ningbo city[17]. Furthermore, industrial activities and vehicular emissions are major PAHs source in the urban industrial and residential areas. For instance, vehicular emission contributes to 56 % of the total PAHs concentration in the urban area of Brisbane Metropolitan Area[35].

The concentration of each species for each sites were displayed in Fig.3. For most PAH congeners, decreasing concentration from industrial (HY and ZH) to rural areas (NUEORS and RY) was observed. The most abundant species were PHE, FLT, FLU, and PYR. The mean concentration (± standard deviation) of PHE, FLT, FLU

7.2 ± 2.5, 11 ± 4.3 for HY; 28 ± 8.6, 9.8 ± 1.8, 8.5 ± 1.2, 5.8 ± 1.0 for ZH; 21 ± 2.2, 9.0 ± 2.6, 6.8 ± 2.3, 5.8 ± 1.6 for UNNC; 26 ± 2.6, 12 ± 1.6, 7.0 ± 1.5, 7.0 ± 1.0 for EMCN; 8.7 ± 2.2, 3.0 ± 1.7, 3.1 ± 1.4, 1.8 ± 0.64 for NUEORS; 11 ± 4.3, 5.0 ± 2.4, 4.0 ±2.0, 2.8 ± 1.1 for RY, respectively. The mean concentration of BaP was 0.09 ± 0.09, 0.16 ± 0.13, 0.10 ± 0.08, 0.10 ± 0.08, 0.11 ± 0.10, 0.04 ± 0.04, 0.07 ± 0.06 for DMS, HY, ZH, UNNC, EMCN, NUEORS and RY, respectively. In generally, higher concentration of PAHs was observed in industrial area.

3.3 Temporal variation of PAHs

Fig. 4a shows the monthly total PAHs (TPAHs) concentration for each site. Different functional area shows different seasonal variation. Strong seasonal variation was found at DMS and HY with high value in winter, while the concentration at NUEORS and RY shows a weak variation. However, the value of PAHs at EMCN and UNNC shows a uniform pattern during the sampling period, where both sites are located in residential area. Moreover, ZH site posed a different seasonal pattern with high concentration in summer that was not observed in other sites. The reason will be discussed later.

The B[a]Peq was investigated in this study. The total mean B[a]Peq was 0.33 ng/m^{3}with a range from 0.04 – 1.10 ng/m^{-3}.The mean ± standard deviation of B[a]Peq for all sites were 0.37 ± 0.32, 0.53 ± 0.28, 0.35 ± 0.17, 0.26 ± 0.13, 0.12 ± 0.08, 0.36 ± 0.17, 0.38 ± 0.18 ng/m^3 for DMS, HY, ZH, RY, NUEORS, UNNC, EMCN respectively. This result was lower than most of research areas, such as Taiyuan[36] (mean ± standard, 27.4 ± 28.1 ng/m^3), Nanjing[37] (range from 0.42 – 1.35 ng/m^3). As shown in Fig.4b, most of the sampling sites shows a light seasonal variation of B[a]Peq with higher value in winter, while lower value in summer.

As it can be seen in Fig.5, the seasonal variation of lPAH for each sites have similar pattern with the seasonal variation of total PAHs shown in Fig.4. The concentrations of mPAH exhibit seasonal variation at DMS, HY, RY and NUEORS with high concentration in winter. Lastly, the pPAH concentrations shows similar seasonal variation at the seven sites with peak concentration in December, 2014. According to previous studies[16, 17], the high value of PAHs in winter could be the result of long range transport of air masses from heavy industrial and biomass burning North China Plain and stagnant weather conditions.

than other sites. Considering the PAHs composition profile, DMS site was characterized by a relatively high value pPAHs (BbF, DBA, IcdP, BghiP) (1.8 ± 1.5 ng/m^3) than the other sites. For DMS site, the most abundant congener was PHE, followed by the FLT, FLU and PYR. This result was in line with previous study with a high value of PHE [16]. Apart from the impacts of regional transport of air masses, DMS site might be greatly impacted by local emission source, such as residents living near the site using coal or biomass burning for heating as above mentioned information.

ZH site shows a different seasonal pattern compares with high PAHs concentration in summer. The PAHs composition profiles at ZH site were also different from other sites. ZH site was characterized by a relatively high proportion of lPAHs (ACY, ACE, FLU) (72%) and low proportion of pPAHs (1.0 %) in the summer. As ZH site was located in an oil refining industrial area, high proporation of lPAH could be the result of oil evaporation, especially in summer with higher temperature. As is known that PAHs are enriched in the oil products. Temperature could influence the partition between gas and particle phase[25]. Higher temperature during the warmer month could drive the PAHs out of condensed particular, such as particles, soil and petroleum products [38]. This can be confirmed by the higher level of lPAHs in summer at ZH in this study. Motelay-Massei et al. [24] also contributes the higher PAHs concentration in the summer in urban areas to the evaporation of petroleum products, such as asphalt, coal tar, roofing tar in Toronto.

3.4 Correspondence analysis (CA)

CA is a multivariate statistical technique, which is commonly used to display a set of data in two-dimensional graphical form, and to visualize the similarities and difference among samples, as well as their main characteristics [39]. In order to characterize the PAH congener profiles associated with each functional district and their temporal variations, three separated CA were performed on the original PAH data set. Although previous studies have already elucidated that LRAT of pollutants from North China Plain and Japan make a contribution to Ningbo areas [16]; and the meteorological parameters, such as temperature and pressure, also have a connection with the concentrations of PAHs [40], this study focuses on discussing the differences and impacts of local sources considering the vicinity of sampling sites.

sites, while the ordination graph was plotted in Fig 6. The first two dimensions accounted for 90.1% of total variance. Dimension 1 was significantly associated with two pPAHs (BkF, BghiP), while dimension 2 was characterized by two lPAHs (ACY, ANT). The origin in the figure corresponds to the centroid of each variable. The closer a variable is to the origin, the closer it is to the average profile. The data points of RY, UNNC and EMCN are more closed to the origin, which indicated the PAH concentrations at these three sites are close to average values. Whereas the other four sites, HY, ZH, DMS and NUEORS, were distinctly separated with each other, and closely associated with PYR, PHE/ACE, DBA and FLU respectively, which revealing they are impacted by different emission source.

Although both located in industrial areas, the PAH congener profiles of HY and ZH are well separated by dimension 1, while ZH has negative value, but HY distributed in positive side. ZH site are associated with PHE and ACE, while HY are frequently associated with BaA and PYR. ZH site have a relatively high proportion of lPAHs (ACY, ACE, PHE, FLU, ANT) (mean: 68 %) and low proportion of pPAHs (mean: 2.1 %), while HY was characterized by a relatively low proportion of lPAHs (mean: 57 %) and high proportion of pPAHs (mean: 3.4 %). As FLU and PYR are dominated in coal combustion [41], the industrial coal combustion released from the power plant at HY might contributes to the high levels of pPAHs. ZH might be impacted by the evaporation of petroleum products as discussed above.

Both located at relatively remote area, the DMS site has a positive loading at Dimension 1, but NUEORS has a negative value. DMS site was more frequently associated with pPAHs (DBA, BbF, IcdP), while NUEORS was frequently associated with FLU. DMS site was characterized by relatively high proportion of pPAHs (mean: 3.7 %) and low proportion of lPAHs (mean: 60 %), while NUEORS have a low proportion of pPAHs (mean: 2.6%) and high proportion of lPAHs (mean: 68 %). Situated on top of mountains, DMS might be influenced by the biomass burning activities in the surrounding countries. Since FLU and PYR are strongly associate with coal combustion [41], NUEORS site might be influenced by domestic coal combustion.

Furthermore, the seasonal variation of PAH congeners were investigated, samples from seven sites were treated as same, while the ordination plot of the months and the chemicals from CA was given in Fig. 7. The first two factors

to the relative abundance of PAHs, the most abundant chemical PHE situated at the rightmost, and from right to left, the corresponding levels of projections of chemicals on dimension 1 keep decreasing. It also shows that the PAH concentrations at Ningbo from February to August are generally at relatively high levels and frequently associated with PHE. PHE is considered to be the result of biomass combustion, particularly from wood combustion [42]. This might suggested that coal/biomass burning are predominate PAHs source in the summer. The dimension 2 is somehow related to the volatility, while the relatively heavier, particle bound PAHs have positive loading and the lighter compounds with negative values. From November to January, the PAHs in Ningbo are significantly influenced by pPAHs (BaP, IcdP, BghiP) and PYR, FLT; and in October, it is strongly linked with lPAHs (ACY, ACE, FLU, ANT) and mPAHs (BkF, CHR, BaA). BaP, IcdP and BghiP are found in diesel and gasoline emissions [43], which suggests diesel/gasoline combustion is one of the major sources of PAHs in Ningbo during the winter time.

Finally, Fig. 8 shows the CA ordination plot between the compounds, the months and the sites. In order to display the data point clearly, we separated the figure into four panels with each panel show the monthly variation of PAH concentrations for no more than two sites. The first two factors accounted for 69.7 % of all the variance. Comparing with previous figure (Fig. 7), it is easy to find that the distribution of PAH congeners in Fig. 8 is extremely similar to the mirror image of that in Fig 7. Thus, we could roughly define that Dimension 2 as the representative of volatility, and the relative abundance decreases along the direction of Dimension 1 here. From February to August, most sites distribute in the left side of the figure associated with PHE with Dimension 1 loadings < 0, which suggests PHE is dominant during summer time. For DMS, UNNC, EMCN, and RY site, the data points of December, November, and January were associated with mPAHs or pPAHs (IcdP, PYR, BghiP). However, for ZH, the data point of December, November, and January were associated with lPAHs (ANT, ACE).

Looking into the monthly distribution of each site in the biplot separately, several points are particularly noteworthy: 1. As suggested in Fig. 6, the points for site UNNC, EMCN and RY are cluster together around the origin. The seasonal change at these three sites generally can reflect the variation of average PAH levels in Ningbo. 2. During the whole sampling period, most points of NUEORS tightly distributed within

NUEORS shows the least temporal variation, and with PHE and FLU as the dominant congeners, which well represents the local background level of PAH pollution. 3. Although both located in industrial area, HY and ZH have totally different PAH congener profile, and are well separated with the two dimensions in the ordination plot. Closing to oil refinery plant, the atmospheric PAHs at ZH show relatively high concentrations with a profile of lPAHs dominant; while HY has lower concentration and higher portion of mPAHs and pPAHs. 5. As the only mountainous site, especially from November to January, DMS shows a congener profile significantly different from others, which is associated with FLT, BbF and PYR. 6. For all sites, the PAH congener profiles in October, which are associated with lPAHs, mostly FLU, ACE and ANT, are significantly differ from other months. October is the harvested season in China, during which the biomass burning of straw and crop residuals could contribute to high levels of pollutants [16]. Satellite image provided in supporting information proved that open fire do occurred intensely in October. However, whether this significant different PAH congener profiles in October might due to the result of biomass burning still need to be further investigated.

3.5 Diagnostic ratio

Diagnostic ratios are widely used to investigate PAH emission source[44]. The value of FLT/(FLT+PYR) ratio suggests different type of source with gasoline (< 0.4), fossil fuel combustion (0.4-0.5) and coal/biomass combustion (> 0.5), respectively. Similarly, the ratio of IcdP/(IcdP+BghiP) suggest pyrogenic (< 0.2), petroleum/gasoline combustion (0.2-0.5) and coal/biomass combustion (> 0.5) [44]. As FLT and PYR are both in gas and solid phase, the pPAHs in PUF samplers are still in linear phase within a short sampling period. Although PUF have a low sampling efficiency for FLT and PYR and may underestimate the concentration of them, here we focus on the seasonal change of diagnostic ratio of FLT/PYR.

Fig. 9 shows the score plot of FLT/(FLT+PYR) against IcdP/(IcdP+BghiP) for all sites. It shows that most of the FLT/(FLT+PYR) ratio are within 0.5-0.75, which suggests biomass/coal combustion; but the value of IcdP/(IcdP+BghiP) varies from 0.3-0.6, which indicates the influence of both petroleum/gasoline combustion and coal/biomass burning. Previous studies, such as Liu et al. [16] and Xu et al [17], also elucidated that coal and biomass burning contributes higher levels of PAHs to Ningbo.

burning.

Fig. 10 and Fig. 11 shows the temporal variation of FLT/(FLT+PYR) and IcdP/(IcdP+BghiP). For most sites, the FLT/(FLT+PYR) values are larger than 0.5; and the IcdP/(IcdP+BghiP) ratios vary from 0.3 to 0.6, which indicate a mix influence of coal/biomass, petroleum/gasoline combustion for PAHs in Ningbo. The higher values of FLT/(FLT+PYR) ratio were found in DMS (mean: 0.67) comparing with other sites, while the lower values were observed in HY (mean: 0.55). The ratios of IcdP/(IcdP+BghiP) also show relatively high values in DMS (mean: 0.46) and lower value in HY (mean: 0.41) as well. These suggest that coal/biomass combustion have relatively stronger influence on mountainous site than others. Moreover, in January and July, the ratios of IcdP/(IcdP+BghiP) for all sites significantly increase from previous months, with ratios larger than 0.5 were observed at DMS, UNNC, EMCN, HY, ZH and RY in July and at DMS and UNNC in January, while the corresponding FLU/(FLU+PYR) ratios are also larger than 0.5. Previous study suggested that rice straw is wildly burned in July in southern China [15]. These imply that the dramatic change of IcdP/(IcdP+BghiP) ratio may due to the biomass combustion.

Interestingly, diagnostic ratios for October did not provide any further indications for the significant different congener profiles founded in the earlier CA results. Although this is due to the fact that the most significant congeners in October (FLU, ACE and ANT) are excluded in the analysis of diagnostic ratios, it highlights the need to identify the important sources for these PAH congeners.

4 Conclusion

We deployed PUF passive air samplers in Ningbo in different functional districts to investigate the temporal and spatial distribution of PAHs and to give insight into potential sources. The total B[a]Peq concentration shows a slight variation with a high value in winter for the sampling sites. The annual average concentrations of PAHs were in the order of industrial district (HY, ZH) ~ urban residential (UNNC, EMCN) > mountain (DMS) > rural areas (RY, NUEORS). Interestingly seasonal variation among the sites was found in this study, which might reflect different emission characterization in different functional areas. In order to identify the corresponding characteristics of their potential sources, correspondence analysis were conducted for these sites with PHE being to be the dominant PAH congener in Ningbo atmosphere

mountain, rural area and residential areas; and even different industrial layout could led to different property of PAH congener emission, while the atmospheric PAHs at area close to oil refinery plant, like ZH, show significant higher portion of light PAHs. There are many evidences indicates that higher concentrations of PAHs at mountain areas during winter time might ascribed to the impacts of local coal/biomass burning. Diagnostic ratios also indicate that both coal/biomass burning and petroleum combustion influence the atmospheric PAHs in Ningbo. PUF-PAS technique was proved to be a useful tool to monitor PAHs in Ningbo. Further analysis still needed to be done to identify the characteristics of potential PAH sources during harvest season.

Acknowledgments

This work was supported by the Knowledge Innovation Program of the Chinese Academy of Sciences (No. IUEQN-2012-03); the National Natural Science Foundation of China (No. 31300435).

Reference:

1. K. H. Kim, S. A. Jahan, E. Kabir and R. J. Brown, *Environ. Int.*, 2013, **60**, 71-80.
2. H. I. Abdel-Shafy and M. S. M. Mansour, *Egyptian Journal of Petroleum*, 2016, **25**, 107-123.
3. N. K. Cheruyiot, W.-J. Lee, J. K. Mwangi, L.-C. Wang, N.-H. Lin, Y.-C. Lin, J. Cao, R. Zhang and G.-P. Chang-Chien, *Aerosol Air Qual. Res.*, 2015, **15**.
4. N. D. Dat and M. B. Chang, *Sci. Total Environ.*, 2017, **609**, 682-693.
5. L. Melymuk, P. Bohlin, O. Sanka, K. Pozo and J. Klanova, *Environ. Sci. Technol.*, 2014, **48**, 14077-14091.
6. F. M. Jaward, N. J. Farrar, T. Harner, A. J. Sweetman and K. C. Jones, *Environ. Toxicol. Chem.*, 2004, **23**, 1355.
7. S.-D. Choi, C. Shunthirasingham, G. L. Daly, H. Xiao, Y. D. Lei and F. Wania, *Environ. Pollut.*, 2009, **157**, 3199-3206.
8. M. Koblizkova, S. Genualdi, S. C. Lee and T. Harner, *Environ Sci Technol*, 2012, **46**, 391-396.
9. G. Q. Liu, G. Zhang, J. Li, X. D. Li, X. Z. Peng and S. H. Qi, *Atmos. Environ.*, 2006, **40**, 3134-3143.
10. X. Zhu, G. Pfister, B. Henkelmann, J. Kotalik, S. Bernhöft, S. Fiedler and K.-W. Schramm, *Environ. Pollut.*, 2008, **156**, 461-466.
11. T. Harner, M. Shoeib, M. Diamond, G. Stern and B. Rosenberg, *Environ. Sci. Technol.*, 2004, **38**, 4474-4483.
12. K. Pozo, T. Harner, S. C. Lee, F. Wania, D. C. Muir and K. C. Jones, *Environ. Sci. Technol.*, 2009, **43**, 796-803.
13. W. J. Hong, H. Jia, W. L. Ma, R. K. Sinha, H. B. Moon, H. Nakata, N. H. Minh, K. H. Chi, W. L. Li, K. Kannan, E. Sverko and Y. F. Li, *Environ. Sci. Technol.*, 2016, **50**, 7163-7174.

Chen, Y. Lu, H. Chen, T. Li, K. Sun, B. Li, W. Liu, J. Liu and S. Tao, *Environ. Sci. Technol.*, 2013, **47**, 6415-6424.
15. Y. Zhang and S. Tao, *Environ. Pollut.*, 2008, **156**, 657-663.
16. D. Liu, Y. Xu, C. Chaemfa, C. G. Tian, J. Li, C. L. Luo and G. Zhang, *Atmo. Pollut. Res.*, 2014, **5**, 203-209.
17. J. S. Xu, H. H. Xu, H. Xiao, L. Tong, C. E. Snape, C. J. Wang and J. He, *Atmos. Res.*, 2016, **178**, 559-569.
18. T. Harner, K. Su, S. Genualdi, J. Karpowicz, L. Ahrens, C. Mihele, J. Schuster, J. P. Charland and J. Narayan, *Atmos. Environ.*, 2013, **75**, 123-128.
19. M. Shoeib and T. Harner, *Environ. Sci. Technol.*, 2002, **36**, 4142-4151.
20. M. Odabasi, E. Cetin and A. Sofuoglu, *Atmos. Environ.*, 2006, **40**, 6615-6625.
21. C. Chaemfa, E. Wild, B. Davison, J. L. Barber and K. C. Jones, *Journal of environmental monitoring : JEM*, 2009, **11**, 1135-1139.
22. J. Klanova, P. Cupr, I. Holoubek, J. Boruvkova, P. Pribylova, R. Kares, T. Tomsej and T. Ocelka, *Journal of environmental monitoring : JEM*, 2009, **11**, 1952-1963.
23. J. He and R. Balasubramanian, in *2012 International Conference on Future Energy, Environment, and Materials, Pt A*, ed. G. Yang, 2012, vol. 16, pp. 494-500.
24. A. Motelay-Massei, T. Harner, M. Shoeib, M. Diamond, G. Stern and B. Rosenberg, *Environ. Sci. Technol.*, 2005, **39**, 5763-5773.
25. S. Liu, S. Tao, W. Liu, H. Dou, Y. Liu, J. Zhao, M. G. Little, Z. Tian, J. Wang, L. Wang and Y. Gao, *Environ. Pollut.*, 2008, **156**, 651-656.
26. L. C. Wang, W. J. Lee, W. S. Lee and G. P. Chang-Chien, *Chemosphere*, 2011, **84**, 936-942.
27. I. C. T. Nisbet and P. K. LaGoy, *Regulatory Toxicology and Pharmacology*, 1992, **16**, 290-300.
28. Y. Lin, X. Qiu, Y. Ma, J. Ma, M. Zheng and M. Shao, *Environ. Pollut.*, 2015, **196**, 164-170.
29. Y. Zhang, Y. Lin, J. Cai, Y. Liu, L. Hong, M. Qin, Y. Zhao, J. Ma, X. Wang, T. Zhu, X. Qiu and M. Zheng, *Sci. Total. Environ.*, 2016, **565**, 994-1000.
30. L. Zhang, W. Yang, L. Dong, S. Shi, L. Zhou, X. Zhang, L. Li, S. Niu and Y. Huang, *Environ. Sci.*, 2013, **34**, 3339-3346.
31. K. Pozo, V. H. Estellano, T. Harner, L. Diaz-Robles, F. Cereceda-Balic, P. Etcharren, K. Pozo, V. Vidal, F. Guerrero and A. Vergara-Fernandez, *Chemosphere*, 2015, **134**, 475-481.
32. Y.-G. Ma, Y. D. Lei, H. Xiao, F. Wania and W.-H. Wang, *Journal of Chemical & Engineering Data*, 2010, **55**, 819-825.
33. P. Bohlin, O. Audy, L. Skrdlikova, P. Kukucka, P. Pribylova, R. Prokes, S. Vojta and J. Klanova, *Environ. Sci. Process Impacts*, 2014, **16**, 433-444.
34. J. Klanova, P. Eupr, J. Kohoutek and T. Harner, *Environ. Sci. Technol.*, 2008, **42**, 550-555.
35. N. Mishra, G. A. Ayoko and L. Morawska, *Environ. Pollut.*, 2016, **208**, 110-117.
36. Z. Xia, X. Duan, S. Tao, W. Qiu, D. Liu, Y. Wang, S. Wei, B. Wang, Q. Jiang, B. Lu, Y. Song and X. Hu, *Environ. Pollut.*, 2013, **173**, 150-156.
37. X. X. Li, S. F. Kong, Y. Yin, L. Li, L. Yuan, Q. Li, H. Xiao and K. Chen, *Atmos. Res.*, 2016, **174**, 85-96.
38. Y. M. Hsu, T. Harner, H. Li and P. Fellin, *Environ. Sci. Technol.*, 2015, **49**, 5584-5592.

H. Wu, *Chemosphere*, 2015, **133**, 22-30.
40. G. Pehnec, I. Jakovljević, A. Šišović, I. Bešlić and V. Vađić, *Atmos. Environ.*, 2016, **131**, 263-268.
41. R. M. Harrison, D. J. T. Smith and L. Luhana, *Environ. Sci. Technol.*, 1996, **30**, 825-832.
42. W. F. Rogge, L. M. Hildemann, M. A. Mazurek, G. R. Cass and B. R. T. Simoneit, *Environ. Sci. Technol.*, 1998, **32**, 13-22.
43. R. K. Larsen and J. E. Baker, *Environ. Sci. Technol.*, 2003, **37**, 1873-1881.
44. M. Tobiszewski and J. Namiesnik, *Environ. Pollut.*, 2012, **162**, 110-119.

Site	Latitude	Longitude	Category	Altitude
DMS	29°52'N	121°31'E	Mountain	446
HY	29°48'N	121°32'E	Industrial	24
ZH	29°53'N	121°46'E	Industrial	15.5
UNNC	29°40'N	121°36'E	Residential	29
EMCN	29°58'N	121°38'E	Residential	43
NUEORS	29°45'N	121°53'E	Rural	0
RY	29°50'N	121°53'E	Rural	0

DMS Da-Mei-Shan; HY Heng-Yang; ZH Zhen-Hai; UNNC University of Nottingham Ningbo, China; EMCN Environment Monitoring Center of Ningbo city; NUEORS Ningbo Urban Environment Observatory and Research Station; RY Rui-Yan.

Table 2 Annual mean concentrations of Σ_{15}PAHs in the seven sites at Ningbo.

Sites	ACY	ACE	FLU	PHE	ANT	FLT	PYR	BaA	CHR	BbF	BkF	BaP	IcdP	DBA	BghiP	Total
DMS	0.2±0.3	0.4±0.5	6.2±4.5	18±9.1	0.2±0.2	9.9±7.5	4.6±3.3	0.2±0.2	1.5±1.2	0.6±0.5	0.4±0.3	0.09±0.1	0.3±0.3	0.1±0.1	0.4±0.4	43±27
HY	1.0±0.7	1.1±0.4	7.3±2.5	27±4.7	0.8±0.4	13±5.6	11±4.3	0.5±0.24	2.0±1.0	0.6±0.2	0.6±0.2	0.2±0.1	0.3±0.2	0.1±0.1	0.5±0.4	66±18
ZH	0.9±0.9	1.4±0.5	8.5±1.2	29±8.4	0.7±0.3	9.8±1.7	5.9±1.1	0.3±0.2	1.1±0.4	0.4±0.1	0.3±0.1	0.1±0.1	0.2±0.1	0.06±0.04	0.3±0.2	58±11
UNNC	0.6±0.6	0.9±0.5	6.9±2.3	21±2.1	0.6±0.4	9.0±2.6	5.8±1.6	0.3±0.2	1.4±0.5	0.5±0.1	0.3±0.1	0.1±0.1	0.2±0.1	0.06±0.04	0.3±0.1	48±9.7
EMCN	0.6±0.6	1.0±0.4	7.0±1.5	26±2.8	0.5±0.3	12±1.5	6.9±1.0	0.4±0.2	1.6±0.5	0.5±0.1	0.3±0.1	0.1±0.1	0.2±0.1	0.07±0.05	0.3±0.2	56±4.6
NUEORS	0.1±0.1	0.4±0.3	3.1±1.5	8.7±2.3	0.1±0.07	3.0±1.7	1.8±0.6	0.1±0.1	0.5±0.2	0.2±0.09	0.1±0.06	0.1±0.1	0.1±0.05	0.02±0.01	0.1±0.1	18±6.9
RY	0.4±0.5	0.4±0.4	4.1±2.1	12±4.4	0.3±0.2	5.0±2.4	2.8±1.1	0.2±0.1	0.8±0.4	0.3±0.1	0.2±0.1	0.1±0.1	0.1±0.1	0.03±0.03	0.2±0.1	27±11

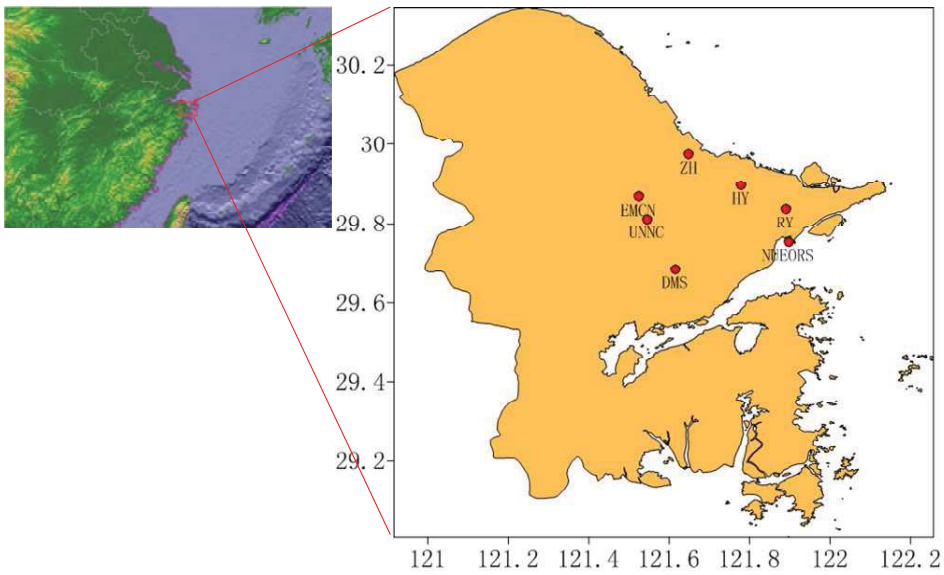
30.2
30
29.8
29.6
29.4
29.2
121
121.2
121.4
121.6
121.8
122
122.2
ZH
HY
RY
EMCN
UNNC
DMS

The upper dot, upper error, upper edge of box, lower edge of box and lower error represent max, 90th, 75th, 25th, 10th. Mean and median are shown in triangle and lines within each box, respectively.

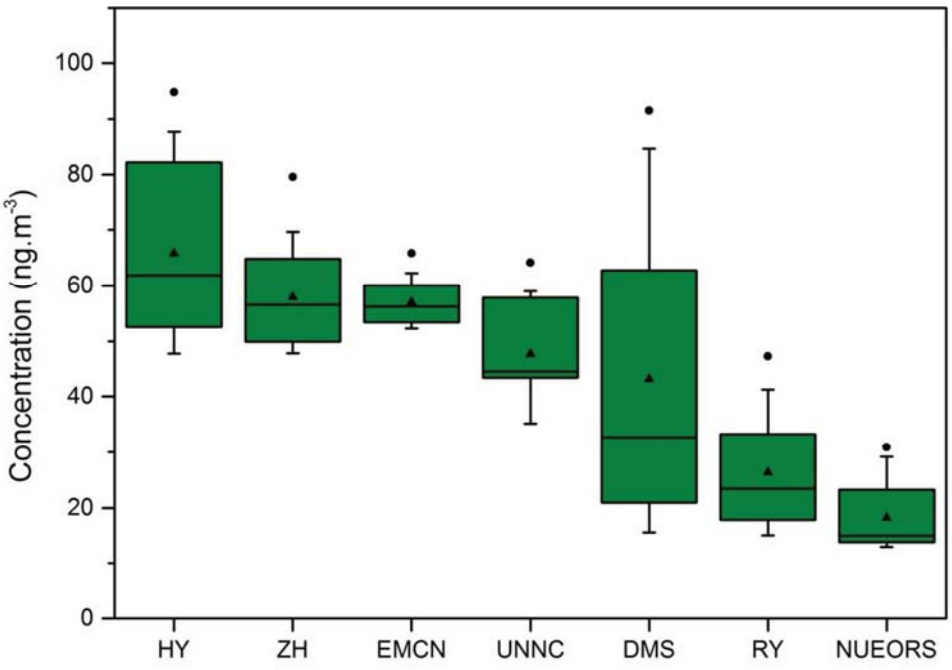

Figure 3 PAH composition profile and its error bar in different sites.

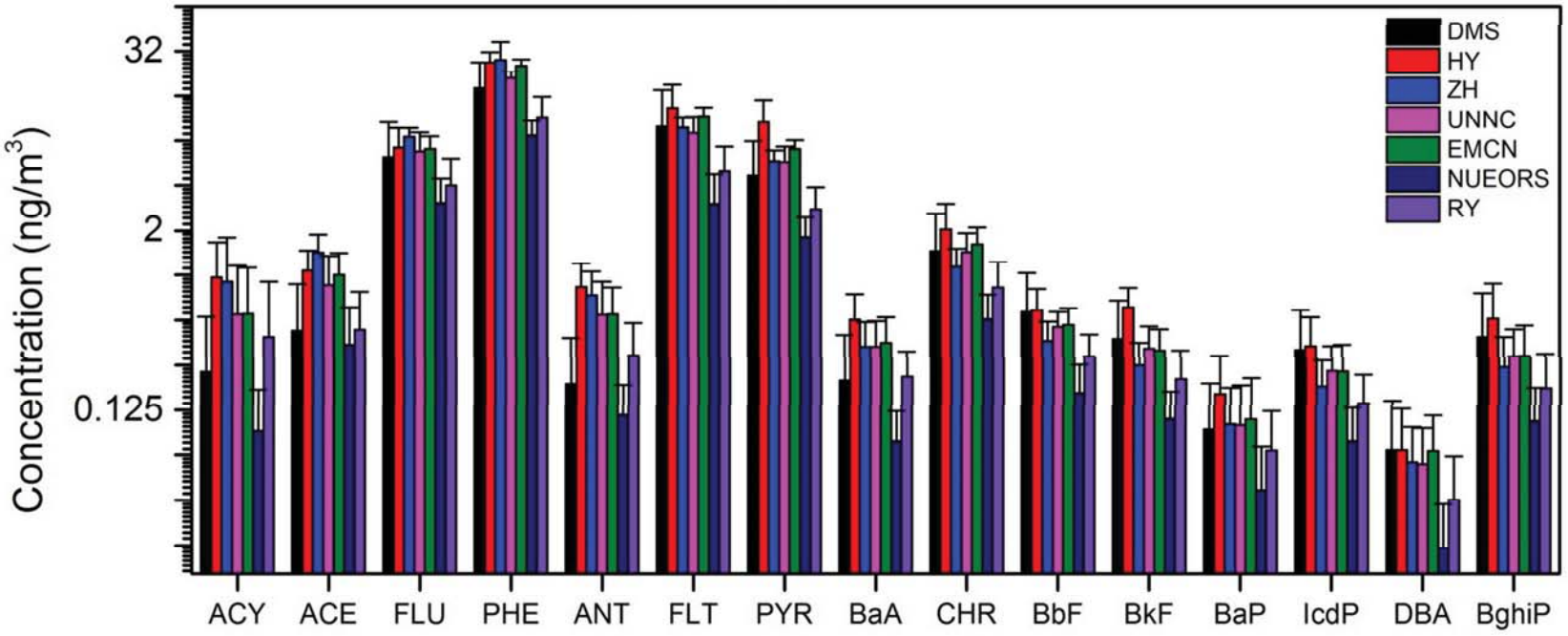

b) for each sites during the sampling period.

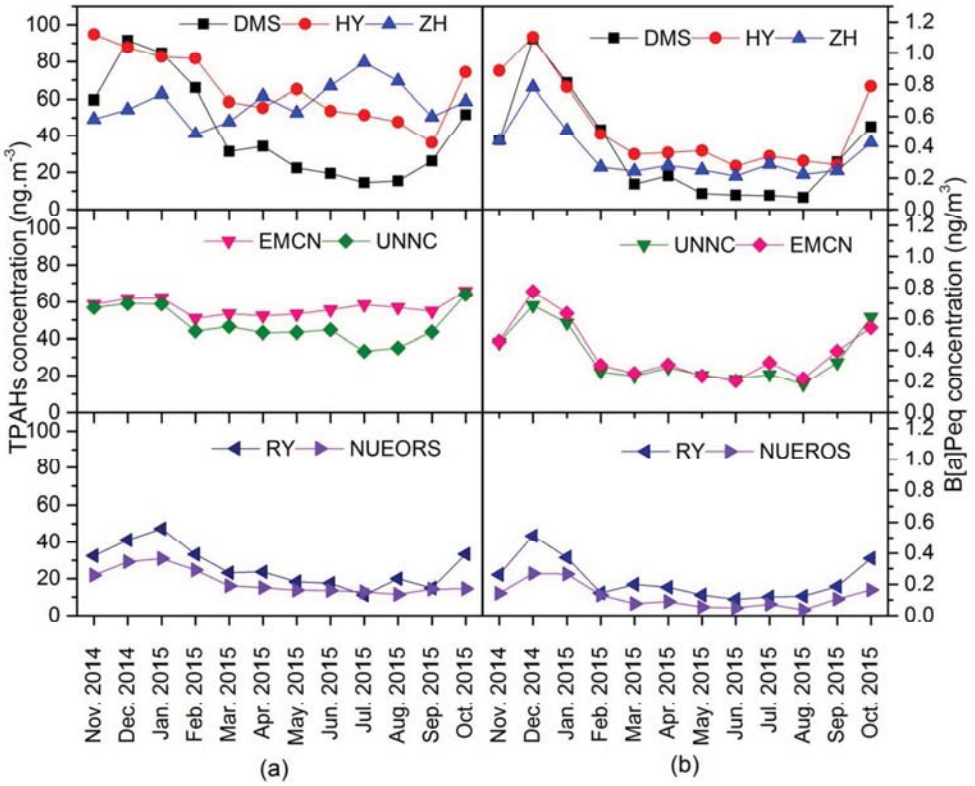

mPAH (middle PAHs, includes FLT, PYR, BaA, CHR), pPAH (particulate PAHs, includes BbF, BkF, BaP, BghiP, IcdP, DBA) at different sites.

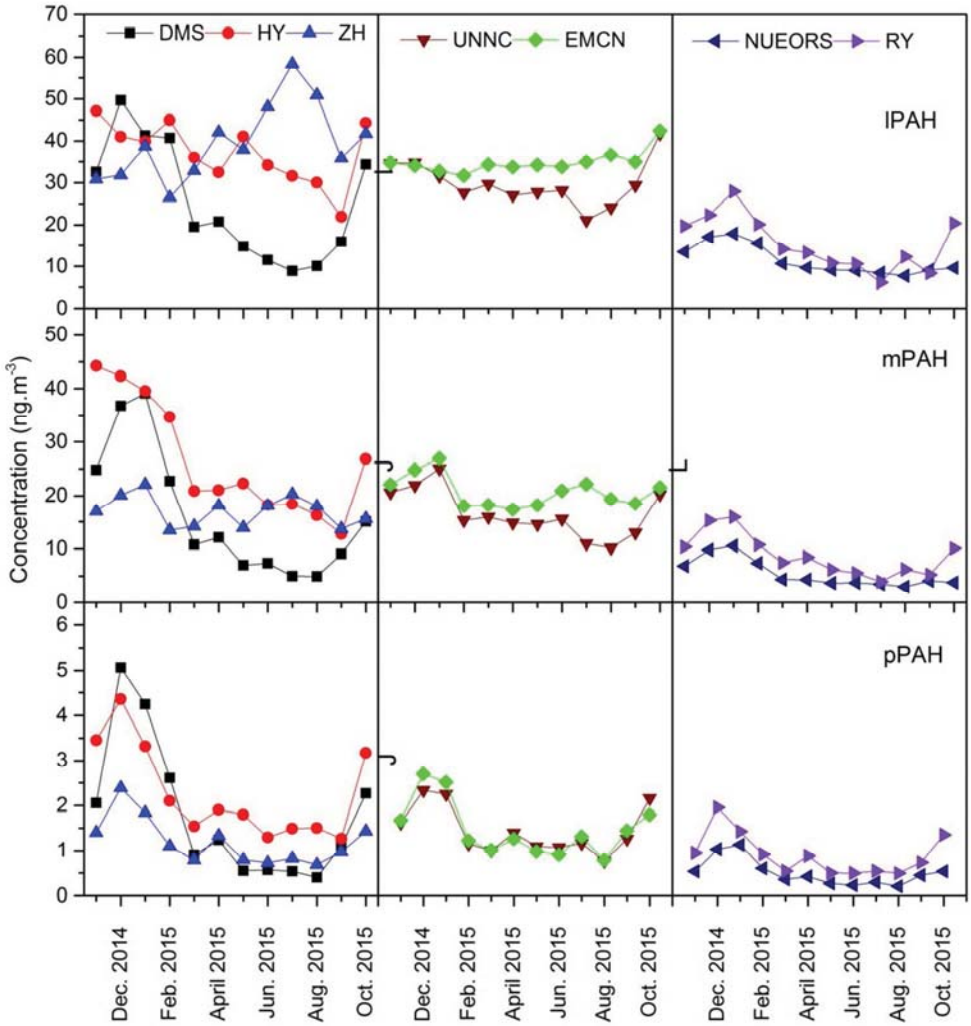

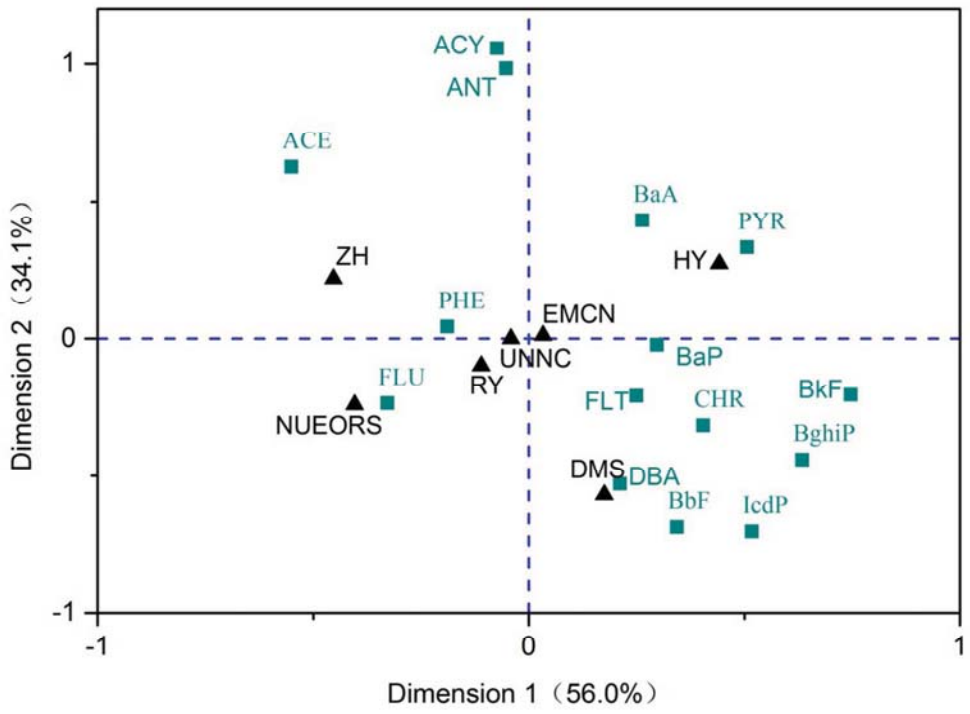
ACY
ANT
ACE
BaA
PYR
ZH
HY
PHE
EMCN
UNNC
BaP
FLU
RY
FLT
CHR
BkF
NUEORS
BghiP
DMS
DBA
BbF
IcdP
1
0
-1
-1
0
1
Dimension 2（34.1%）
Dimension 1（56.0%）

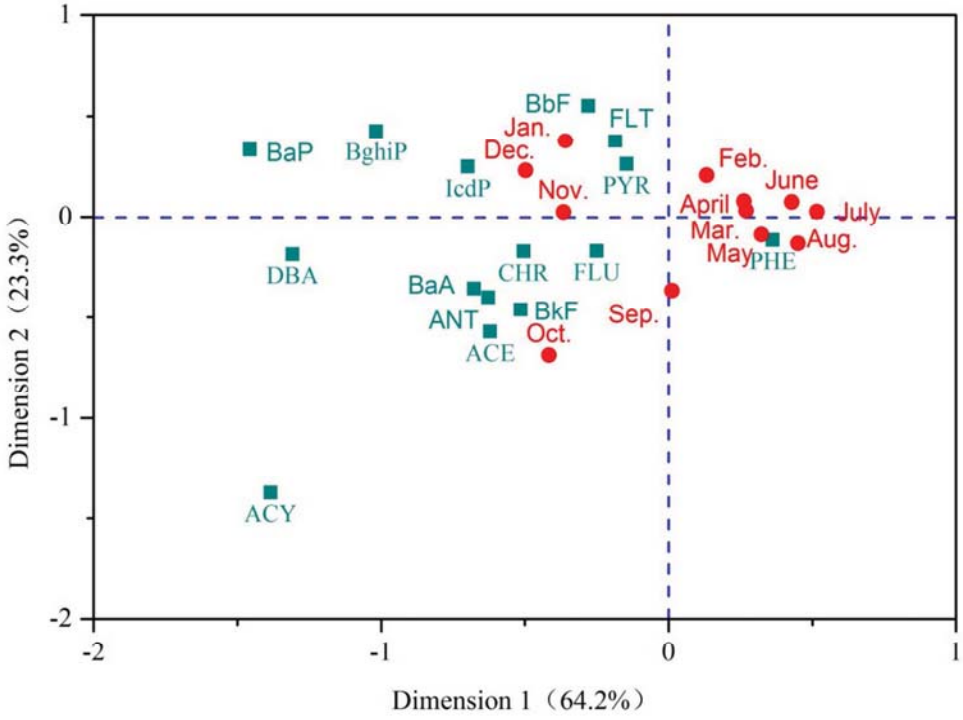
BbF
FLT
Jan.
BaP
BghiP
Dec.
Feb.
June
IcdP
Nov.
PYR
April
July
Mar.
Aug.
May
PHE
DBA
CHR
FLU
BaA
ANT
BkF
Sep.
Oct.
ACE
ACY
1
0
-1
-2
-2
-1
0
1
Dimension 2（23.3%）
Dimension 1（64.2%）

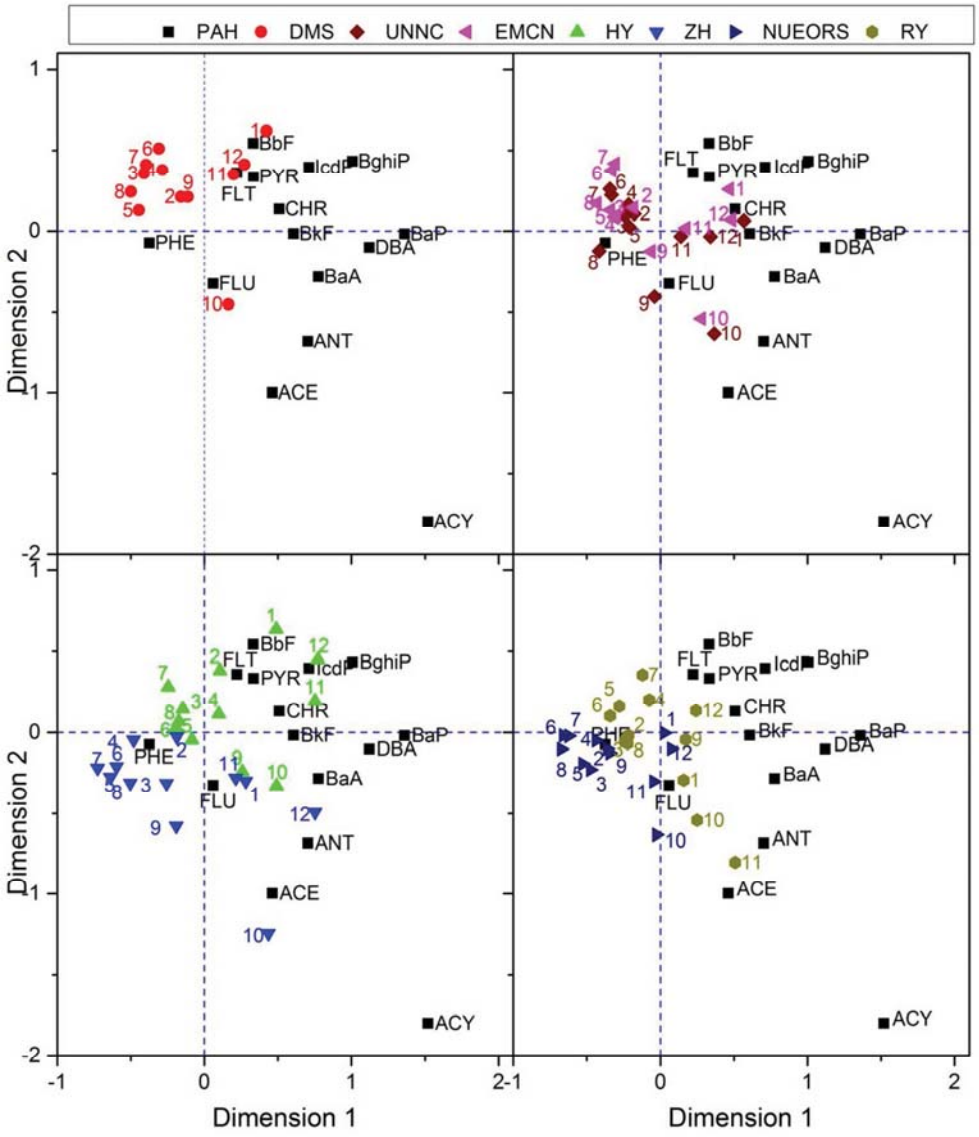
PAH
DMS
UNNC
EMCN
HY
ZH
NUEORS
RY
BbF
FLT
PYR
IcdP
BghiP
CHR
BkF
BaP
DBA
PHE
FLU
BaA
ANT
ACE
ACY
Dimension 1
Dimension 2

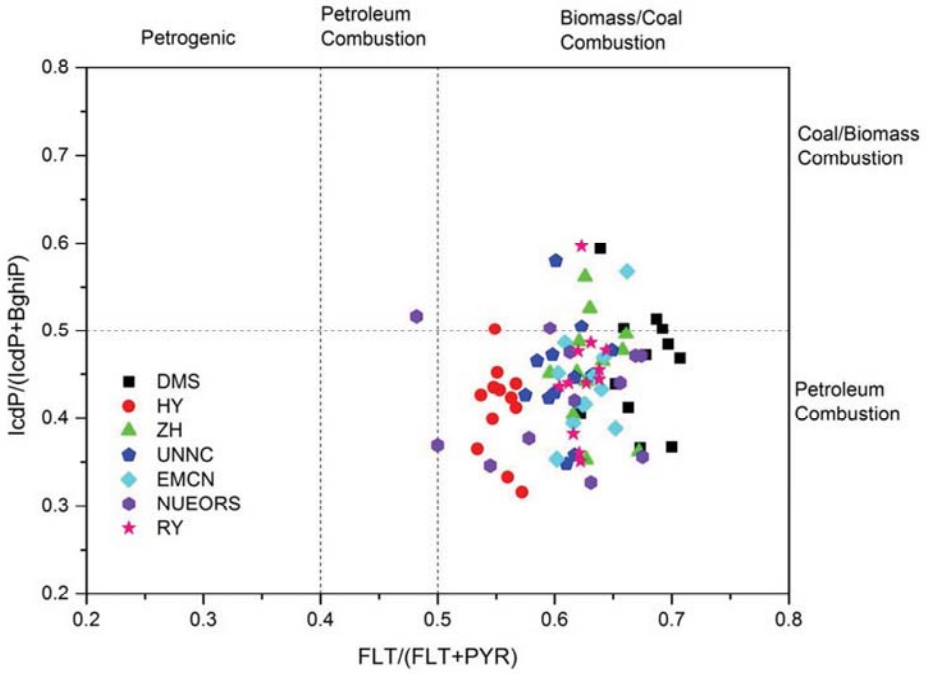
Petrogenic
Petroleum Combustion
Biomass/Coal Combustion
Coal/Biomass Combustion
Petroleum Combustion
IcdP/(IcdP+BghiP)
FLT/(FLT+PYR)
DMS
HY
ZH
UNNC
EMCN
NUEORS
RY
0.2
0.3
0.4
0.5
0.6
0.7
0.8

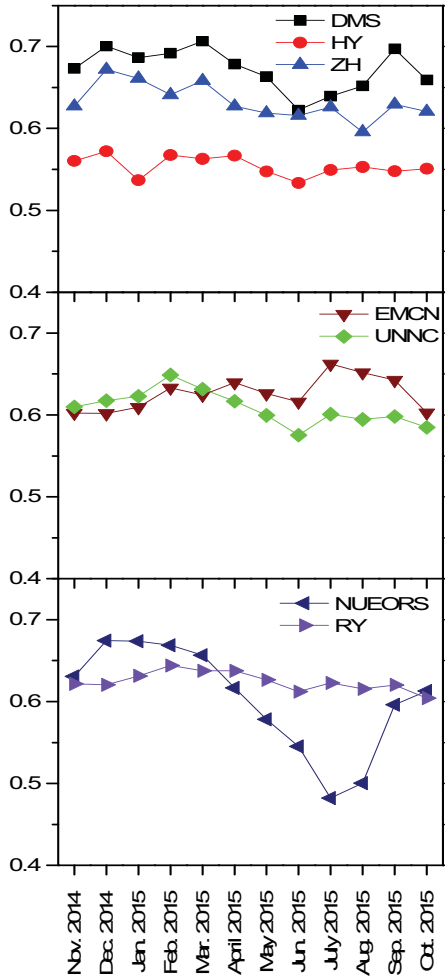
DMS
HY
ZH
EMCN
UNNC
NUEORS
RY
0.7
0.6
0.5
0.4
Nov. 2014
Dec. 2014
Jan. 2015
Feb. 2015
Mar. 2015
April 2015
May 2015
Jun. 2015
July 2015
Aug. 2015
Sep. 2015
Oct. 2015

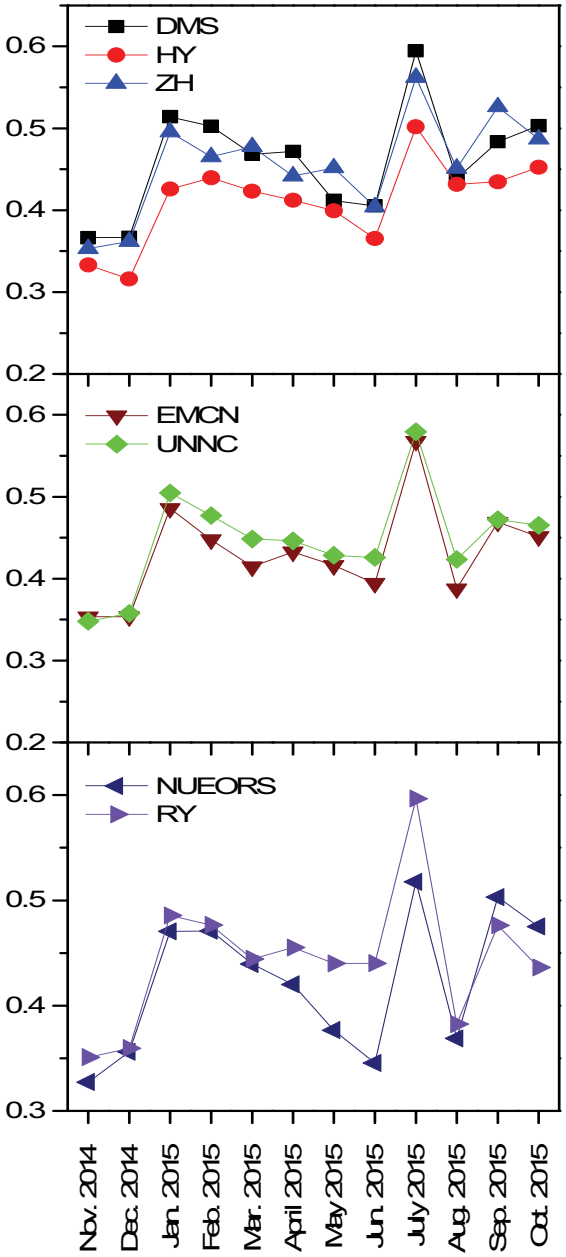
DMS
HY
ZH
EMCN
UNNC
NUEORS
RY
0.6
0.5
0.4
0.3
0.2
Nov. 2014
Dec. 2014
Jan. 2015
Feb. 2015
Mar. 2015
April 2015
May 2015
Jun. 2015
July 2015
Aug. 2015
Sep. 2015
Oct. 2015

Associated with Functional districts in Ningbo, China

Cheng-Hui Peng[1,2,3,a], Lei Tong[1,3,a], Zhong-Wen Huang[1,2,3], Jing-jing Zhang[1,2,3], Hang Xiao[1,3*], Neng-Bin Xu[4], Jun He[5]

[1] Center for Excellence in Regional Atmospheric Environment, Institute of Urban Environment, Chinese Academy of Sciences, Xiamen 361021, China

[2] University of Chinese Academy of Sciences, Beijing 100049, China

[3] Ningbo Urban Environment Observation and Research Station-NUEORS, Chinese Academy of Sciences, Ningbo 315830, China

[4] Environment monitoring Center of Ningbo, Ningbo 315012, China

[5] University of Nottingham Ningbo China, Ningbo 315100, China

[*]Correspondence author: Hang Xiao

Center for Excellence in Regional Atmospheric Environment,

Institute of Urban Environment, Chinese Academy of Sciences

1799 Jimei Avenue, Xiamen, China, 361021

E-mail address: hxiao@iue.ac.cn

Tel: + 86 574 8678 4813

a. The two authors contributed equally to this paper.

List of Figures

	EMCN	NUEORS
Nov. 2014	14.1	15.7
Dec. 2014	7.4	7.4
Jan. 2015	7.9	7.7
Feb. 2015	8.5	7.7
Mar. 2015	12.2	10.4
Apr. 2015	18.2	15.0
May 2015	22.2	19.2
June 2015	26.2	23.3
July 2015	24.0	25.2
Aug. 2015	27.8	26.8
Sep. 2015	24.9	24.0
Oct. 2015	21.1	20.3

Table S2 Atmospheric concemtration of 15 PAHs in different districs in Ningbo

Site	Month	ACY	ACE	FLU	PHE	ANT	FLT	PYR	BaA	CHR	BbF	BkF	BaP	IcdP	DBA	BghiP	TPAH
DMS	Nov.2014	0.58	0.62	7.68	23.23	0.19	14.57	7.08	0.23	2.93	0.62	0.46	0.09	0.29	0.10	0.51	59.17
DMS	Dec.2014	0.31	0.57	14.60	33.61	0.41	22.41	9.58	0.62	4.12	1.40	0.99	0.30	0.78	0.27	1.34	91.30
DMS	Jan.2015	0.52	1.27	11.42	28.69	0.43	24.86	11.35	0.48	2.39	1.52	0.82	0.22	0.81	0.11	0.77	85.68
DMS	Feb.2015	0.11	1.08	10.43	29.86	0.24	14.52	6.47	0.27	1.49	0.90	0.49	0.13	0.52	0.08	0.51	67.09
DMS	Mar.2015	0.04	0.01	3.58	15.50	0.06	7.05	2.93	0.08	0.70	0.34	0.18	0.03	0.16	0.02	0.18	30.86
DMS	Apr.2015	0.04	0.14	4.06	16.17	0.08	7.50	3.55	0.07	0.96	0.50	0.29	0.04	0.18	0.02	0.21	33.82
DMS	May2015	0.03	0.09	3.32	11.03	0.07	4.33	2.20	0.04	0.46	0.21	0.11	0.02	0.09	0.01	0.13	22.13
DMS	June2015	0.01	0.07	2.27	9.31	0.03	4.24	2.57	0.03	0.56	0.27	0.13	0.01	0.07	0.01	0.10	19.66
DMS	July2015	0.04	MDL	1.27	7.55	0.04	2.82	1.59	0.05	0.51	0.20	0.08	0.01	0.15	0.02	0.10	14.42
DMS	Aug.2015	0.002	MDL	2.04	8.04	0.04	2.87	1.54	0.03	0.49	0.15	0.07	0.01	0.07	0.02	0.09	15.45
DMS	Sep.2015	0.09	0.23	3.47	12.06	0.08	5.28	2.29	0.09	1.41	0.27	0.25	0.11	0.20	0.07	0.21	26.12
DMS	Oct.2015	0.94	1.03	10.69	21.07	0.61	8.68	4.49	0.36	1.55	0.43	0.62	0.17	0.47	0.10	0.47	51.69
HY	Nov.2014	2.29	1.67	12.08	29.60	1.26	22.11	17.34	0.80	3.96	0.85	0.79	0.30	0.46	0.15	0.91	94.58
HY	Dec.2014	1.51	1.34	9.44	27.44	1.07	21.45	16.04	0.81	3.96	0.95	0.78	0.43	0.63	0.21	1.36	87.46
HY	Jan.2015	0.43	1.15	9.39	28.66	1.30	19.85	17.13	0.66	1.88	0.86	0.51	0.31	0.66	0.09	0.89	83.79
HY	Feb.2015	0.88	1.34	7.85	35.28	0.74	18.18	13.86	0.47	2.16	0.75	0.51	0.12	0.30	0.05	0.39	82.88
HY	Mar.2015	0.32	0.93	6.84	27.13	0.46	10.77	8.36	0.34	1.38	0.47	0.42	0.09	0.22	0.04	0.31	58.09
HY	Apr.2015	0.99	0.92	5.18	24.59	0.50	10.86	8.30	0.27	1.61	0.64	0.62	0.08	0.22	0.03	0.32	55.14
HY	May2015	0.94	1.00	7.00	30.82	0.94	11.28	9.32	0.34	1.41	0.44	0.85	0.09	0.17	0.02	0.25	64.86
HY	June2015	0.40	1.10	6.47	25.77	0.64	9.01	7.87	0.26	1.08	0.37	0.48	0.06	0.14	0.02	0.24	53.91
HY	July2015	0.18	0.34	4.11	26.17	0.81	9.03	7.41	0.49	1.42	0.38	0.33	0.07	0.34	0.05	0.34	51.47
HY	Aug.2015	0.44	0.75	4.75	23.53	0.53	8.06	6.51	0.30	1.38	0.42	0.54	0.07	0.19	0.03	0.26	47.76
HY	Sep.2015	1.10	0.63	4.04	15.80	0.33	6.03	4.98	0.30	1.47	0.27	0.47	0.07	0.18	0.04	0.24	35.94
HY	Oct.2015	2.14	1.76	9.80	29.20	1.43	12.77	10.42	0.95	2.71	0.62	1.03	0.24	0.52	0.12	0.63	74.34
ZH	Nov.2014	0.53	1.78	8.03	20.15	0.85	9.27	6.12	0.42	1.80	0.41	0.31	0.16	0.18	0.08	0.33	50.41
ZH	Dec.2014	2.02	1.79	8.11	19.96	1.33	11.31	7.48	0.63	2.04	0.58	0.47	0.31	0.36	0.18	0.66	57.23
ZH	Jan.2015	1.59	1.73	9.39	26.00	1.12	12.38	7.93	0.53	1.27	0.60	0.31	0.19	0.34	0.06	0.36	63.79
ZH	Feb.2015	0.08	1.19	6.54	18.65	0.35	7.62	4.41	0.26	0.80	0.36	0.20	0.08	0.18	0.04	0.23	40.99
ZH	Mar.2015	0.44	1.35	7.02	23.10	0.63	8.19	4.93	0.24	0.81	0.29	0.17	0.08	0.10	0.03	0.14	47.51
ZH	Apr.2015	0.20	0.94	7.94	28.87	0.30	9.50	5.35	0.21	1.01	0.45	0.28	0.08	0.15	0.03	0.20	55.50
ZH	May2015	0.48	0.98	8.55	31.07	0.54	9.24	5.52	0.20	0.83	0.36	0.20	0.07	0.11	0.03	0.15	58.33
ZH	June2015	0.39	1.17	9.57	36.47	0.69	10.55	6.58	0.18	0.80	0.31	0.18	0.04	0.08	0.01	0.12	67.15
ZH	July2015	0.57	0.98	9.68	46.42	0.80	12.63	6.44	0.25	0.96	0.25	0.12	0.04	0.20	0.08	0.15	79.57
ZH	Aug.2015	0.35	1.30	10.03	37.52	0.61	10.70	5.71	0.21	0.86	0.22	0.14	0.04	0.09	0.03	0.14	67.97
ZH	Sep.2015	1.14	1.47	7.55	24.64	0.45	7.70	4.28	0.30	1.11	0.22	0.26	0.06	0.17	0.03	0.19	49.55
ZH	Oct.2015	3.10	2.54	9.84	25.01	1.24	8.24	5.43	0.57	1.38	0.32	0.39	0.11	0.24	0.08	0.29	58.78

UNNC	Nov.2014	0.36	1.22	9.48	22.57	0.74	10.93	6.99	0.40	2.30	0.44	0.34	0.14	0.22	0.09	0.41	56.61
UNNC	Dec.2014	0.46	1.39	9.71	21.78	1.19	11.96	7.41	0.51	2.02	0.55	0.41	0.27	0.35	0.14	0.63	58.79
UNNC	Jan.2015	1.59	1.17	8.07	20.99	0.82	14.40	8.73	0.48	1.44	0.72	0.40	0.23	0.44	0.06	0.43	59.95
UNNC	Feb.2015	0.15	0.94	6.90	20.32	0.29	9.17	4.96	0.21	0.95	0.40	0.24	0.07	0.20	0.03	0.22	45.06
UNNC	Mar.2015	0.29	0.45	6.40	21.86	0.33	9.23	5.38	0.21	1.07	0.37	0.23	0.06	0.15	0.02	0.18	46.22
UNNC	Apr.2015	0.25	0.51	5.17	20.59	0.24	8.24	5.12	0.19	1.24	0.53	0.35	0.08	0.19	0.03	0.23	42.95
UNNC	May2015	0.59	0.36	4.98	21.19	0.35	7.92	5.29	0.21	1.16	0.45	0.26	0.05	0.14	0.02	0.19	43.15
UNNC	June2015	0.05	0.58	5.25	22.10	0.32	8.20	6.05	0.19	1.15	0.50	0.26	0.03	0.11	0.01	0.15	44.97
UNNC	July2015	0.15	0.12	3.08	17.44	0.33	5.70	3.79	0.35	1.17	0.39	0.17	0.03	0.31	0.05	0.23	33.29
UNNC	Aug.2015	0.11	0.57	5.31	18.44	0.26	5.50	3.75	0.24	0.93	0.31	0.18	0.02	0.12	0.03	0.16	35.93
UNNC	Sep.2015	0.62	1.21	7.16	19.91	0.47	6.56	4.41	0.35	1.65	0.32	0.37	0.06	0.21	0.07	0.23	43.61
UNNC	Oct.2015	1.96	1.86	10.79	25.92	1.23	10.17	7.22	0.67	2.17	0.46	0.65	0.19	0.35	0.11	0.40	64.13
EMCN	Nov.2014	0.63	1.24	8.31	22.81	0.64	11.66	7.10	0.39	2.16	0.43	0.34	0.15	0.22	0.08	0.40	56.55
EMCN	Dec.2014	0.72	1.46	8.52	21.20	1.06	13.12	8.02	0.60	2.23	0.63	0.47	0.31	0.38	0.17	0.67	59.55
EMCN	Jan.2015	0.99	1.25	8.19	21.79	0.79	15.20	8.87	0.52	1.50	0.77	0.40	0.25	0.45	0.09	0.48	61.54
EMCN	Feb.2015	0.14	1.05	7.36	23.66	0.48	10.81	5.97	0.26	1.01	0.43	0.23	0.09	0.21	0.03	0.23	51.99
EMCN	Mar.2015	0.17	0.84	6.58	24.40	0.35	10.05	5.71	0.21	1.06	0.34	0.20	0.07	0.14	0.03	0.17	50.32
EMCN	Apr.2015	0.32	0.74	6.69	26.95	0.29	10.68	6.07	0.18	1.35	0.51	0.33	0.08	0.19	0.03	0.22	54.64
EMCN	May2015	0.30	0.67	5.87	24.97	0.33	9.92	5.91	0.15	1.09	0.38	0.21	0.05	0.11	0.04	0.15	50.15
EMCN	June2015	0.10	0.67	5.70	27.16	0.33	11.99	7.60	0.16	1.24	0.45	0.23	0.03	0.09	0.01	0.12	55.87
EMCN	July2015	0.20	0.35	4.21	29.70	0.47	12.40	7.51	0.44	1.83	0.50	0.21	0.03	0.30	0.07	0.21	58.43
EMCN	Aug.2015	0.18	0.68	6.07	29.40	0.34	10.81	6.75	0.24	1.52	0.30	0.18	0.03	0.10	0.03	0.16	56.79
EMCN	Sep.2015	0.71	1.32	6.95	25.56	0.40	9.96	6.10	0.38	2.07	0.34	0.37	0.06	0.26	0.12	0.29	54.90
EMCN	Oct.2015	2.10	1.78	9.67	27.87	1.00	11.35	7.43	0.60	2.16	0.42	0.55	0.16	0.24	0.10	0.31	65.77
RY	Nov.2014	1.59	0.77	5.62	12.55	0.32	5.60	3.33	0.21	1.24	0.27	0.21	0.09	0.12	0.04	0.23	32.19
RY	Dec.2014	0.21	0.53	6.95	15.13	0.38	8.52	4.16	0.34	1.71	0.49	0.36	0.20	0.28	0.11	0.49	39.86
RY	Jan.2015	1.28	0.98	7.65	21.27	0.58	9.93	5.09	0.31	1.11	0.51	0.26	0.13	0.27	0.04	0.28	49.70
RY	Feb.2015	0.15	0.40	3.47	11.12	0.16	4.55	2.55	0.13	0.56	0.27	0.16	0.04	0.10	0.01	0.11	23.79
RY	Mar.2015	0.21	0.53	5.32	16.06	0.23	6.58	3.41	0.18	0.78	0.37	0.18	0.05	0.14	0.02	0.15	34.21
RY	Apr.2015	0.21	0.31	3.33	11.59	0.25	4.74	2.82	0.16	0.65	0.30	0.18	0.06	0.11	0.02	0.14	24.86
RY	May2015	0.11	0.16	2.68	9.08	0.17	3.74	2.30	0.11	0.54	0.25	0.14	0.04	0.08	0.01	0.09	19.50
RY	June2015	0.04	0.15	2.47	8.39	0.12	3.25	2.03	0.10	0.45	0.21	0.11	0.03	0.06	0.004	0.09	17.52
RY	July2015	0.05	MDL	1.01	5.40	0.12	2.10	1.25	0.16	0.43	0.18	0.08	0.02	0.14	0.03	0.11	11.06
RY	Aug.2015	0.01	0.19	3.12	9.68	0.51	3.33	2.26	0.23	0.60	0.19	0.13	0.02	0.07	0.02	0.09	20.43
RY	Sep.2015	0.24	0.22	1.95	6.62	0.10	2.76	1.63	0.20	0.77	0.19	0.22	0.05	0.13	0.04	0.12	15.24
RY	Oct.2015	0.61	1.10	5.82	13.69	0.63	5.28	3.22	0.41	1.17	0.30	0.44	0.12	0.21	0.06	0.22	33.29
NUEORS	Nov.2014	0.25	0.57	3.77	9.49	0.17	3.76	2.20	0.08	0.78	0.16	0.12	0.04	0.07	0.03	0.13	21.61
NUEORS	Dec.2014	0.15	0.67	5.57	11.53	0.18	5.79	2.79	0.16	1.04	0.28	0.21	0.10	0.14	0.05	0.26	28.94
NUEORS	Jan.2015	0.09	0.89	5.98	12.94	0.30	6.55	3.17	0.17	0.70	0.38	0.18	0.10	0.21	0.03	0.24	31.93

NUEORS	Feb.2015	0.15	0.54	4.49	12.47	0.10	4.53	2.24	0.08	0.53	0.23	0.14	0.03	0.09	0.02	0.11	25.76
NUEORS	Mar.2015	0.04	0.29	2.70	8.06	0.04	2.60	1.36	0.05	0.31	0.15	0.08	0.02	0.05	0.01	0.07	15.83
NUEORS	Apr.2015	0.02	0.14	2.40	7.48	0.06	2.40	1.49	0.04	0.36	0.15	0.10	0.03	0.06	0.01	0.08	14.83
NUEORS	May2015	0.04	0.17	2.07	7.16	0.10	1.96	1.43	0.04	0.30	0.11	0.06	0.01	0.03	MDL	0.06	13.56
NUEORS	June2015	0.04	0.14	2.12	7.53	0.08	1.89	1.57	0.03	0.27	0.11	0.05	0.01	0.03	MDL	0.05	13.91
NUEORS	July2015	0.04	MDL	1.51	7.38	0.14	1.45	1.55	0.08	0.39	0.09	0.04	0.01	0.08	0.01	0.07	12.85
NUEORS	Aug.2015	0.04	0.03	1.63	6.53	0.07	1.29	1.29	0.05	0.36	0.08	0.05	0.007	0.03	MDL	0.05	11.49
NUEORS	Sep.2015	0.06	0.20	2.12	7.27	0.11	2.06	1.39	0.08	0.60	0.11	0.15	0.02	0.08	0.02	0.08	14.34
NUEORS	Oct.2015	0.22	0.52	2.96	6.51	0.08	1.99	1.25	0.07	0.46	0.11	0.16	0.08	0.08	0.02	0.09	14.60

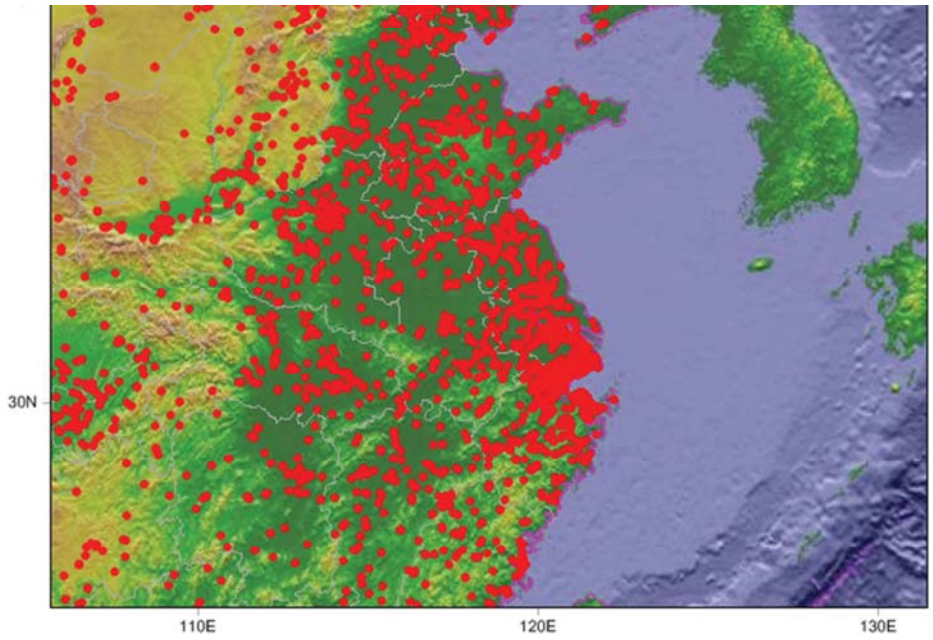
30N
110E
120E
130E

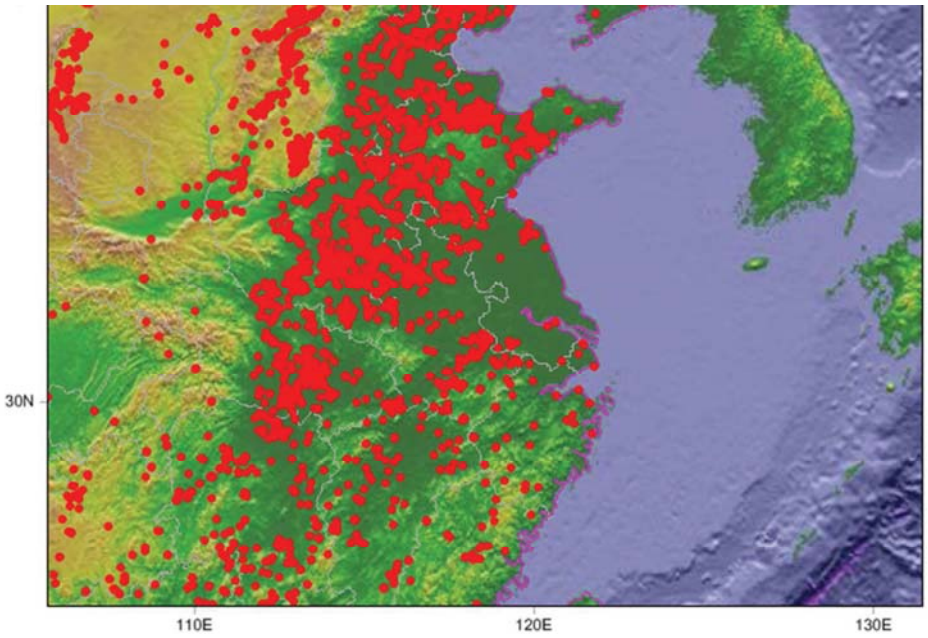
30N
110E
120E
130E